Current Topics in Toxicology
Vol. 10, 2014

Original Communication

Characterization of functionalized nanodiamonds and their effects on cell viability and gene expression in human lung epithelial cells

Abebe E. Mengesha[1,*], Miezan J. Ezoulin[2], Tao Zhang[2], Karin Gaudenz[3], Christopher Seidel[4], Valery Khabashesku[4], James Murowchick[5] and Bi-Botti Celestin Youan[2]

[1]College of Pharmacy & Health Sciences, Drake University, Des Moines, IA 50311, [2]School of Pharmacy, University of Missouri-Kansas City, MO 64108, [3]Stowers Institute for Medical Research, Kansas City, MO 64110, [4]Department of Chemical and Biomolecular Engineering, University of Houston, TX 77204, [5]Department of Geological Science, University of Missouri-Kansas City, MO 64110, USA.

ABSTRACT

The increasing application of nanodiamond and its derivatives in many industries and healthcare products warrants a critical and urgent need to elucidate potential adverse effects. This study evaluated the cell viability and gene expression patterns of human lung epithelial cell line (Calu-3) exposed to nanodiamond (ND) and 4 surface functionalized nanodiamonds (SF-NDs): glycine-ND (Gly-ND); glucose-ND (Glu-ND); fluorinated-ND (F-ND) and ethylenediamine-ND (EDA-ND). The ND and SF-NDs were characterized using X-ray diffraction (XRD), scanning electron microscopy (SEM), dynamic light scattering (DLS) and attenuated total reflectance Fourier transformed infrared (ATR-FTIR) spectrum. The cytotoxicity of ND and SF-NDs was evaluated using MTS assay. Gene expression profiles were generated using microarray analysis for Calu-3 cells exposed to ND. The results of XRD and ATR-FTIR spectra provided evidence for successful functionalization of ND. The morphological and particle size analysis using SEM and DLS revealed that ND and SF-NDs form agglomeration. The cytotoxicity study data showed that ND and SF-NDs exhibit concentration dependent material-specific toxicity with the general trend for biocompatibility: Gly-ND > Glu-ND > ND > F-ND > EDA-ND. Microarray analysis indicated a subtle cellular response to ND with few genes affected more than 2-fold up or down. However, some gene expressions such as NAD(P)H dehydrogenase (*NQO1*) showed up-regulation while a gene associated with the metastasis of lung adenocarcinoma transcript 1 (*MALAT1*) was down-regulated. In conclusion, at the concentrations of < 100 µg/mL, ND and SF-NDs appeared to be safe to human lung epithelial cells *in vitro* after 24 hrs exposure.

KEYWORDS: nanodiamond, surface functionalized nanodiamonds, cytotoxicity, gene expression profile, Calu-3 cells

INTRODUCTION

There is an emerging research interest toward nanodiamonds (ND) and surface functionalized-NDs (SF-NDs) for controlled and targeted drug delivery [1-4], imaging probe [5], cellular biosensors and biomarkers [6-8], and implant coating in biological systems [9]. However, in recent years, several epidemiologic studies reported deleterious health effects of not only airborne particles [10-16] but also specifically carbonaceous particulate matter which can have serious implications for children [17, 18] and patients with pulmonary diseases such as asthma and pneumonia [19-21].

*Corresponding author: abebe.mengesha@drake.edu

Therefore, there are legitimate concerns related to safe handling of nanomaterials [22-25].

Nanodiamonds with a modified surface offer the most significant potential for biological and medical applications [9]. The fabrication of biologically amenable functionalized nanomaterials provides a platform for safe delivery of biomimetic and therapeutically active substrates [26]. In the category of nanoparticles, carbon based nano-materials have been one of the most extensively used and industrially manufactured because of their unique and superior properties that combine extreme hardness, chemical inertness, high adsorption capacity and high specific surface area [27]. Synthetic diamond is formed using high-pressure, chemical-vapor-deposition and shock-wave, detonation [28-30] or conversion of silicon carbide to crystalline diamond-structured carbon at ambient pressure [31]. Recently, advanced ND-mediated vehicles for localized and systemic drug/gene delivery were reported [1, 2, 32-39]. In addition, the surface of ND is readily derivatized with various functional groups for either covalent or non-covalent conjugation with biomolecules [36, 40-42] that improve the adsorption as well as translocation through various biological barriers. Modified diamond nanowires were found to produce an electrical response on binding to DNA [43] warranting the need for in-depth assessment of the biological responses of ND and SF-NDs intended for any industrial application. Recently, several ND based materials were assessed towards this goal [44-48].

One of the requirements for ND and SF-NDs to be an effective drug delivery tool is the absence of remarkable cytotoxicity. Even though studies with ND demonstrated that they are well tolerated by various cell types [49, 50] and animals [51], recent investigation reported a DNA damage in embryonic stem cells induced by ND [22]. These clearly indicate that further examination of toxicity of ND and SF-NDs is needed. Further, the surface modification of ND might introduce a considerable amount of potentially toxic impurities, which are not completely removed during purification.

The aim of this study was to characterize the physicochemical properties of ND and SF-NDs and investigate the cytotoxicity of ND and 4 SF-NDs, at the concentration range 0.01-1000 μg/mL using a human lung epithelial cell line (Calu-3). In addition, the gene expression profile in ND-exposed Calu-3 was assessed using Affymetrix GeneChip Human Genome U133 Plus 2.0 Arrays.

MATERIALS AND METHODS

Materials

Nanodiamond (ND) powder (3-6 nm, purity 97%, < 2.5% graphite and amorphous carbon, 0.1-0.15% Fe, 0.1-0.3% Si) was purchased from Nanostructured and Amorphous Materials, Inc. (Houston, TX, USA). Aqueous suspensions of ND (average particle size 4 nm, 4% and 10% concentrations) were purchased from Plasma Chem GmbH (Berlin, Germany). Fe, Zn, Cu and Mn impurities were in trace amounts. Surface functionalized-ND samples (SF-NDs) with covalently attached moieties, glycine-ND (Gly-ND), glucose-ND (Glu-ND), fluorinated-ND (F-ND) and ethylenediamine-ND (EDA-ND) were synthesized and provided by Dr. Khabashesku's research group [52].

Physicochemical characterization of ND and SF-NDs

ND and SF-NDs were characterized using X-ray diffraction (XRD), scanning electron microscopy (SEM), dynamic light scattering (DLS), and attenuated total reflectance Fourier transformed infrared (ATR-FTIR) spectroscopy. XRD data were collected on Miniflex automated X-ray diffractometer (Rigaku, The Woodland, TX, USA) at room temperature. Co Kα radiation was set at 2° 2θ/min. X-ray data were used for the fingerprint characterization of crystalline structure of the ND and SF-NDs. ATR-FTIR spectroscopy was used to determine the functional groups in the ND and SF-NDs that confirm the successful surface functionalization of ND [52]. The ATR-FTIR spectral measurements were carried out using a Thermo Nicolet Nexus 870 FTIR system (Thermo Nicolet, Madison, WI, USA) with an ATR accessory.

The aggregation and surface morphology of the ND and SF-NDs were characterized using SEM and DLS. Samples were prepared by placing 5 μL of the ND and SF-NDs aqueous suspension onto a 300 mesh carbon-coated copper grid and allowing the samples to settle for 3-5 min. The excess fluid was removed by wicking it off with an absorbent paper. Samples were negatively stained in 1%

aqueous solution of uranyl acetate for 5 min and were analyzed on SEM (FEGESEMXL 30, FEI, Hillsboro, OR, USA). Pictures were taken using a digital camera (Gatan axis-mount 2kx2k). The particle size and size distribution of ND and SF-NDs were measured using DLS (90 Plus, Particle Size Analyzer, Brookhaven Instruments Corporation, Holtsville, NY, USA). About 1% w/v suspension of ND and SF-NDs were prepared in water and the mean particle diameter, size distribution and polydispersity index (PI) were measured. The temperature and laser wavelength were set at 25 °C and 450 nm, respectively. A refractive index of 1.344 was used. DLS measurements were conducted in triplicate and results were presented as mean ± standard deviation (SD).

Cytotoxicity assay

Calu-3 cell line was purchased from American Type Culture Collection (ATCC, Manassas, VA, USA) and grown in DMEM media supplemented with 10% FBS at 37 °C, 5% CO_2. Ninety-six well plates were seeded with 20,000 cells per well and incubated for 2 hr at 37 °C, in humidified incubator with 5% CO_2. Cells were then exposed to ND or SF-NDs at the concentration range 0.01-1000 µg/mL for 24 hr. The ND and SF-NDs were dispersed in the culture medium and sonicated prior to addition to the cells. Medium-treated cells were used as controls. The concentration of ND and SF-NDs was selected based on the calculated surface area of ND in the 96 well plates.

The Brunauer Emmett Teller (BET) surface area based on the monolayer molecular adsorption of the ND is 340 m^2/g and hence 0.1 µg of ND will form a monolayer on the surface of each well having surface area of 0.35 cm^2. Accordingly, the concentrations of ND and SF-NDs in the range of 0.01 to 1000 µg/mL could be expressed in terms of surface area as 0.035 to 3500 cm^2/mL. Before the cytotoxicity assay, the dosing solutions were aspirated, cell lines were washed three times and 100 µL DMEM medium added to each well. Cell viability was assessed by adding 20 µL of MTS (3-(4,5-dimethylthiazol-2-yl)-5-(3-carboxy-methoxyphenyl)-2-(4-sulfophenyl)-2H-tetrazolium) reagent (Promega, Madison, WI) and incubating at 37 °C for 2 hr. The absorbance was then measured at 450 nm using ELISA plate reader (DTX 880, Beckman Coulter Inc., Brea, CA, USA) with multimode detection software. Data was converted to % viability and results analyzed using ANOVA and Bonferroni's Multiple Comparison Test to assess statistical significance. Values of $p < 0.05$ were considered statistically significant. The cells morphology was analyzed using light microscopy (Vistavision, VWR Inc., West Chester, PA, USA).

Gene expression analysis

Microarray data for gene expression profiling was acquired using the Affymetrix Human Genome U133 Plus 2.0 GeneChip system. To characterize gene expression profiles, Calu-3 cells were exposed to ND at a concentration of 100 µg/mL in a T75 flask for three days. For comparison, a parallel control sample was prepared in which ND were omitted. Total RNA was extracted from both samples and purified with a RNeasy kit (Qiagen) using a method reported previously [53]. Briefly, Calu-3 cells were homogenized in TRIZOL reagent (Gibco BRL) following the manufacturer's instructions and the TRIZOL-isolated RNA were further purified with RNeasy kit and resuspended in DEPC-treated water (Sigma-Aldrich). Gene expression arrays used in this experiment are Affymetrix GeneChip Human Genome U133 Plus 2.0 Arrays. These consist of probe sets designed for analysis of over 47,000 transcripts based on sequences from GenBank, dbEST, and RefSeq.

The procedure was conducted according to the manufacturer's instructions by using One-Cycle Target Labeling and Control Reagents (Affymetrix) for cDNA synthesis, purification, and the synthesis of biotin-labeled cRNA. Ten µg fragmented cRNA was hybridized to a Human Genome U133 Plus 2.0 Arrays for 18 hr at 45 °C at 60 rpm, after which the array was washed, stained and scanned using Gene Array Scanner (Affymetrix). The digital image files were processed by Affymetrix Microarray and converted into base10 logarithmic values. Then, these values were normalized and reversed into non-logarithmic values by calculating their exponential numbers in decimal. The ratio of gene expression for cells exposed to ND compared to a control was calculated as shown in Eq. 1.

$$M = \log_2 \left(\frac{\text{Gene expression of ND exposed cells}}{\text{Gene expression of control cells}} \right) \quad \text{(Eq. 1)}$$

Genes were ranked by their "M value" that indicates the degree of up- or down-regulation.

RESULTS AND DISCUSSION

Characterization of ND and SF-NDs

Scanning electron micrographs (SEM) of the ND and SF-NDs showed agglomerates of fine particles (Figure 1a-e). It is noteworthy that contrary to aggregates, agglomerates are reversible, and agglomerates of ND may be redispersed and stabilized as shown in the aqueous ND samples. The images of cloudy and fluffy material depicted the nature of the loose agglomerates formed by the ND. The SF-NDs showed relatively larger agglomerates, which was consistent with the DLS results. Table 1 shows the mean particle diameter and the PI of the ND and SF-NDs. The aqueous and colloidal dispersions of 4 and 10% concentration ND samples showed 40 and 83 nm average size particles, respectively, while the powder ND and the SF-NDs showed relatively large size particles (at micron level) due to the formation of agglomerations. It has been observed that dispersion of nanomaterials in solution rarely leads to distribution at the primary particle size [54]. The 4 and 10% ND samples which are suspended and stabilized by surfactants showed minimal agglomeration during the DLS measurements. Moreover, the powder ND and SF-NDs exhibited heterogeneous nature as indicated by the PI. This agglomeration raises concerns when considering the size-dependent toxicity. The need to characterize nanoparticles in solution before assessing the toxicity has been reported [54]. Murdock *et al.* found the use of DLS to evaluate the toxicological effect observed due to agglomeration changes in the presence of serum or cell culture media. In this study, in order to reduce the degree of agglomeration, ND and SF-ND samples were sonicated in the culture media before exposing cell lines for cytotoxic evaluation [54].

The X-ray diffraction (XRD) of 10% aqueous suspension of ND taken after drying showed the characteristic peaks of the positively charged ND at 2θ around 51°, 90° and 112° (Figure 2a). The SF-NDs showed identical XRD pattern indicating that the surface derivatization of the ND did not affect its crystalline structure. Figure 2b illustrates the XRD of EDA-ND as an example for SF-NDs. Absence of other peaks in the SF-NDs pattern implies that the derivatization did not produce a crystalline layer on the surface of the ND.

Figure 3 depicts the ATR-FTIR spectrum of the NDs and the 4 SF-NDs. The ATR-FTIR spectrum of the ND (Figure 3a) exhibits a strong absorption at 3420 cm^{-1}, medium-intensity shoulder peaks in the 2800-3000 cm^{-1} region, and bands between 1750-1000 cm^{-1} due to the O–H, C–H, C═O, C═C, and C–O stretching and bending deformation modes of the hydroxyl, carboxylic acid and the anhydride, carbonyl, CH, and C═C surface functional groups. The ATR-FTIR spectra of the SF-NDs (Figure 3b Gly-ND; Figure 3c Glu-ND; Figure 3d F-ND; and Figure 3e EDA-ND) were significantly different from the spectrum of ND (Figure 3a) indicating successful surface modifications. The ATR-FTIR spectrum of Gly-ND (Figure 3b) showed typical features of a covalently attached glycine amino acid in the range typical for the zwitterionic structure for the moiety ($–NH_2^+CH_2COO^–$) [55] with N–H stretches at 3280 and 3088 cm^{-1} and carboxylate anion stretches at 1642 and 1554 cm^{-1}. The absorption due to the O–H stretches at 3420 cm^{-1} in the ND (Figure 3a) and in Glu-ND (Figure 3c) samples is virtually absent in the spectrum of the F-ND (Figure 3d). Instead, strong peaks were observed in the C–F stretch region in between 1340 and 900 cm^{-1}. In the spectrum of EDA-ND (Figure 3e), a broad peak at 3360-3400 cm^{-1} and a medium-intensity peak at 1630 cm^{-1} may be related to the N–H stretches and NH_2 scissor motion, respectively, of the *N*-ethyleneamino group attached to the ND surface.

Cytotoxicity study

Figure 4 depicts the % viability of Calu-3 cells after 24 hr exposure to various concentrations of ND and SF-NDs. The bioreduction of MTS dye into a colorful formazan product occurs only in viable cells with functional mitochondria. The % cell viability was calculated from the reduction of the MTS dye in comparison to the media-treated cells (control). As shown in the figure, ND and SF-NDs induced a concentration dependent material-specific cytotoxicity. Up to a concentration of 10 μg/mL, ND and SF-NDs reduced cell viability to about 80% ($p < 0.05$). At concentration of

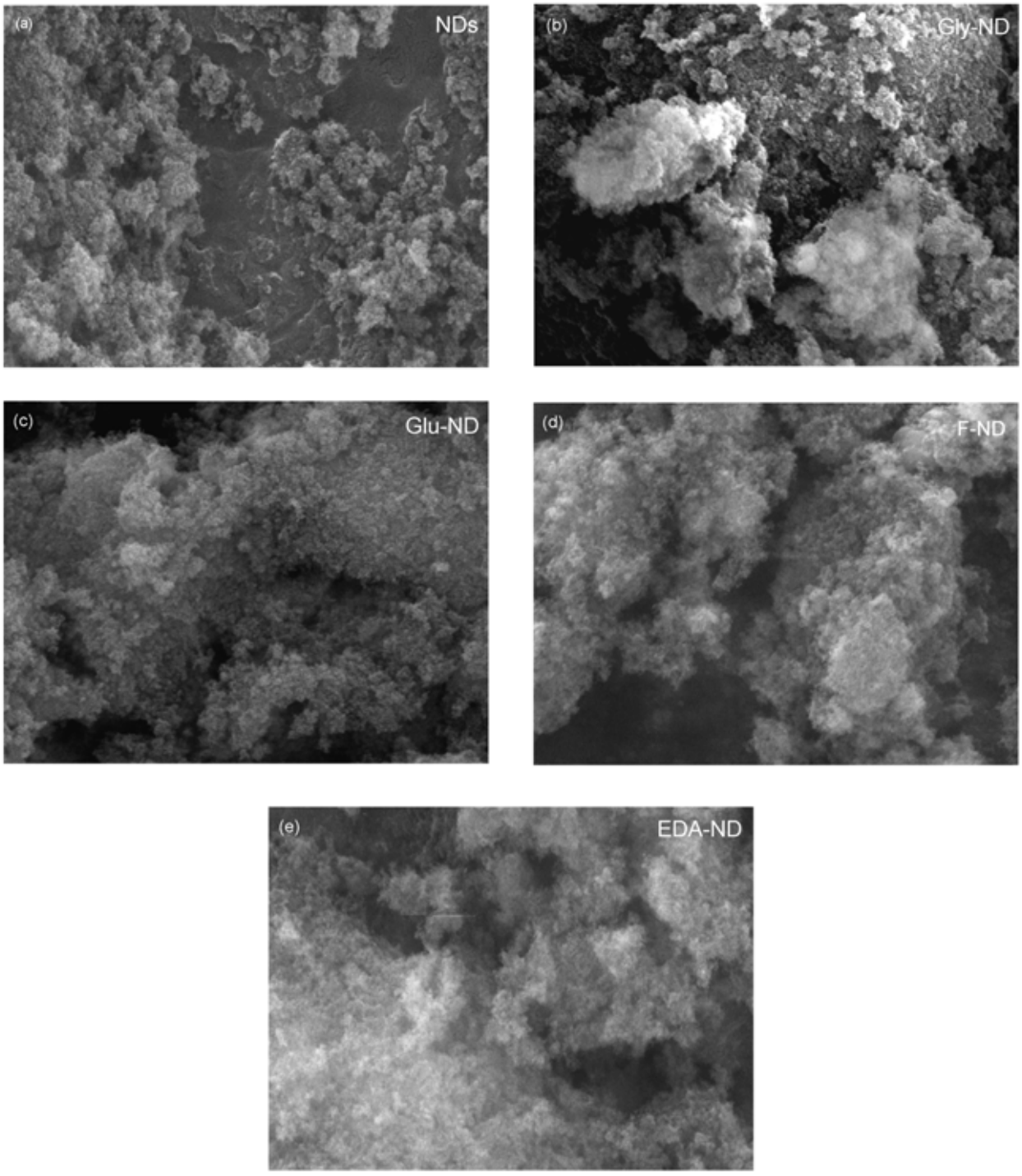

Figure 1. Scanning electron micrograph of a) ND; b) Gly-ND; c) Glu-ND; d) F-ND; and e) EDA-ND.

100 μg/mL, EDA-ND markedly decreased the cell viability to about 70% ($p < 0.05$). At the highest concentration studied, 1000 μg/mL, ND and SF-NDs significantly reduced cell viability. At this concentration, EDA-ND was found to be the most cytotoxic with 22% cell viability, while Gly-ND was the least cytotoxic with 54% cell viability. The percent cell viability for Glu-ND, native ND

Table 1. Mean diameter and the polydispersity of NDs and the surface functionalized NDs.

Samples	Diameter* Mean (nm) ± S.D.	Polydispersity index
4% Nanodiamond	39.8 ± 0.6	0.005
10% Nanodiamond	83.8 ± 2.4	0.005
Powder Nanodiamond	479.9 ± 36	0.055
Gly-ND	1554.2 ± 56	0.244
Glu-ND	553.3 ± 72	0.273
F-ND	1276.1 ± 108	0.348
EDA-ND	1703.0 ± 62	0.247

*n = 3; S.D. = standard deviation.

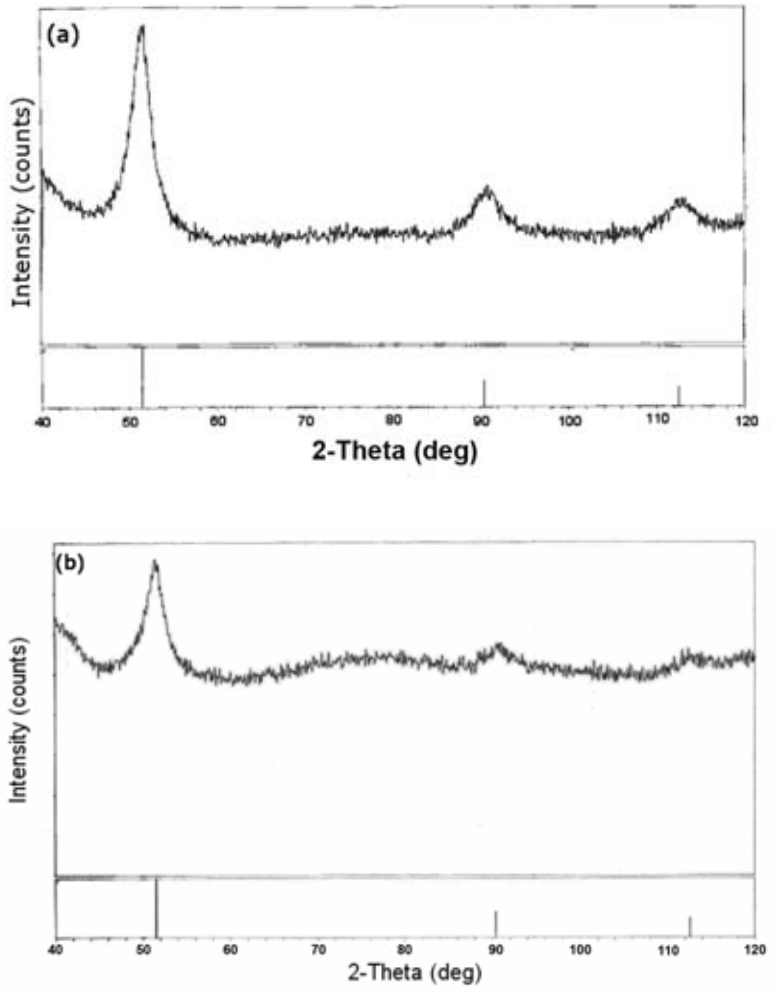

Figure 2. X-ray diffractions of a) 10% ND dispersion (PL-D-G01P) and b) EDA-ND.

and F-ND was found to be 42, 39 and 34%, respectively. Based on the cytotoxicity results at 1000 μg/mL, the order of biocompatibility of the samples was as follows: Gly-ND > Glu-ND > ND > F-ND > EDA-ND.

The interference of ND with the colorimetric cytotoxic assay has been frequently raised [49]. Various approaches were recommended including centrifugation of the samples to remove the ND, selective extraction of the colorimetric reagent

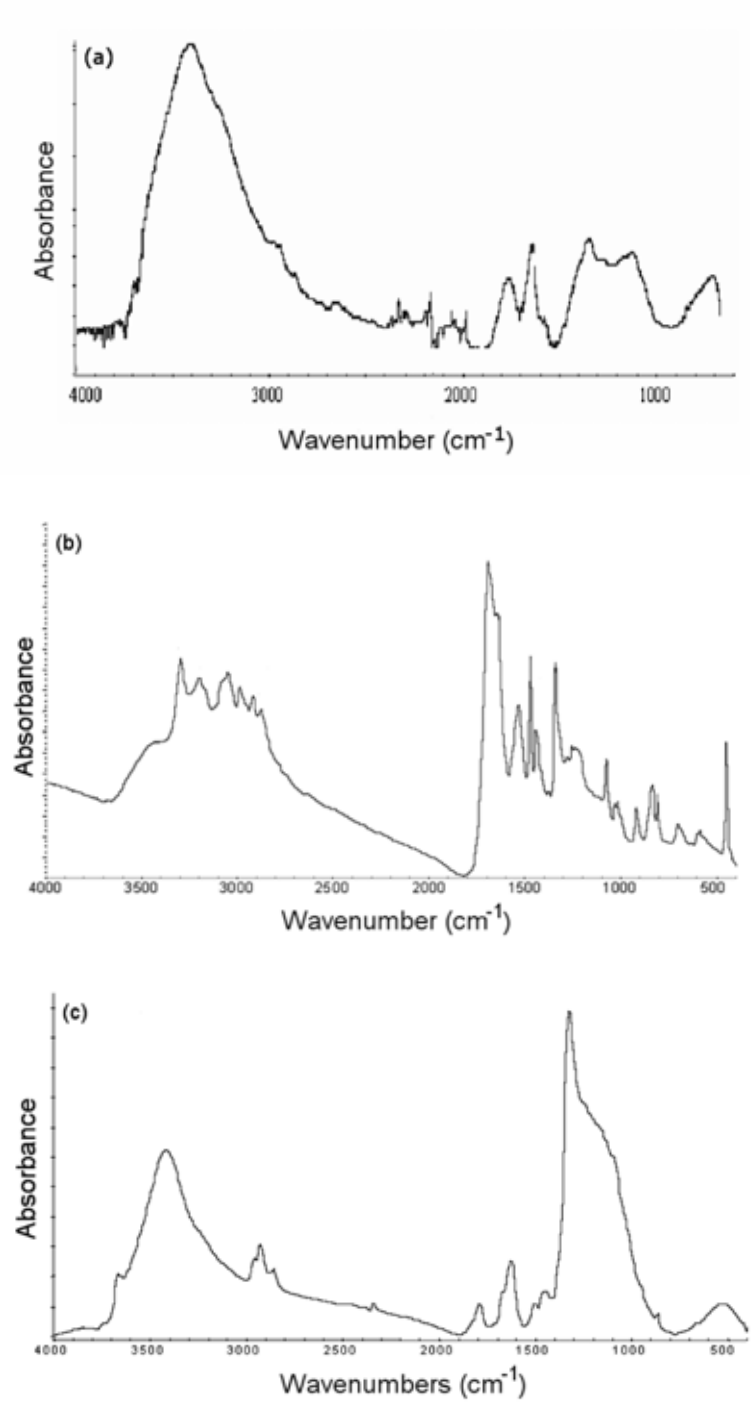

Figure 3

Figure 3 continued..

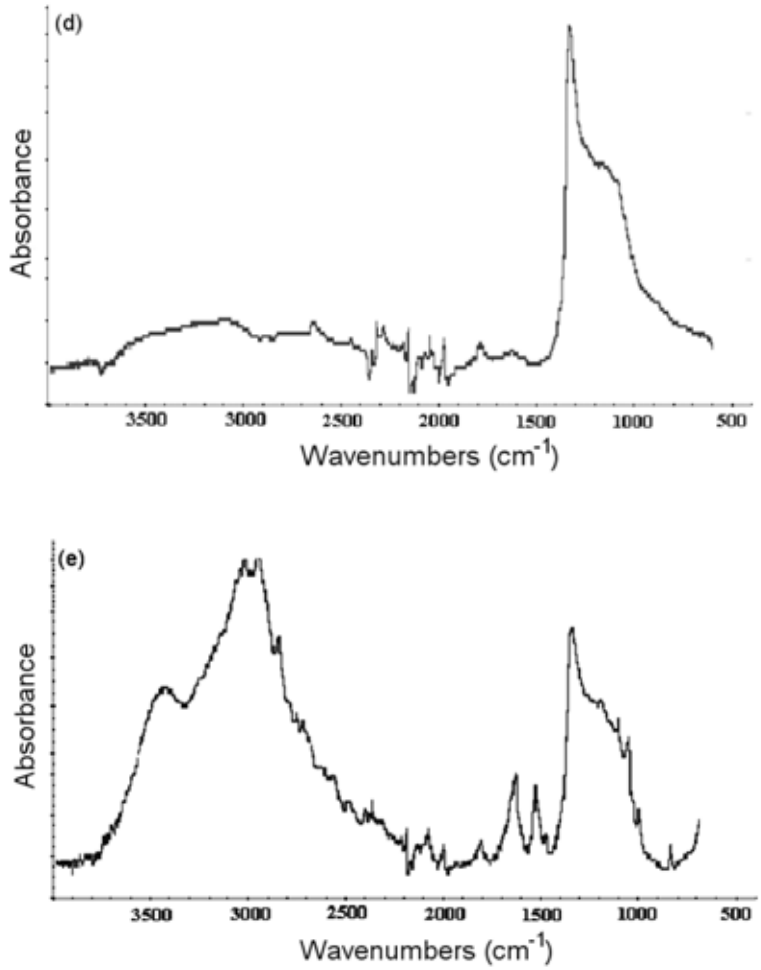

Figure 3. ATR-FTIR spectrum of a) ND; b) Gly-ND; c) Glu-ND; d) F-ND; and e) EDA-ND.

using appropriate solvent and optimization of the optical conditions in which ND display lower interference. In this study, most of the ND and SF-ND samples were removed by aspiration followed by washing before adding the MTS reagent. This procedure significantly reduced the ND and SF-NDs interference.

Figure 5 shows the morphology of Calu-3 cells exposed to ND and SF-NDs at the concentration of 1000 μg/mL. After 24 hr exposure, cells showed different morphology compared to control (Figure 5a). Cells incubated with EDA-ND (Figure 5f) and F-ND (Figure 5e) displayed more rounded structures which are morphological indicators of cytotoxicity. This result is in a good agreement with the MTS assay (Figure 4) where EDA-ND and F-ND showed 22 and 34% cell viability, respectively. Large agglomerates of the ND and SF-NDs were visible in the field (Figure 5) which might alter the cytotoxicity results. This might be due to the high concentration of the samples which might promote agglomeration.

Taking the BET surface area of the ND into consideration, the 1000 μg/mL concentration is equal to 0.34 m^2 which can make up to 10,000 monolayers in each well of the 96 well plates. Such a high concentration of ND may induce indirect cytotoxicity by medium depletion. Casey *et al.* [56] reported that single-walled carbon nanotubes at high concentration bind to sugars,

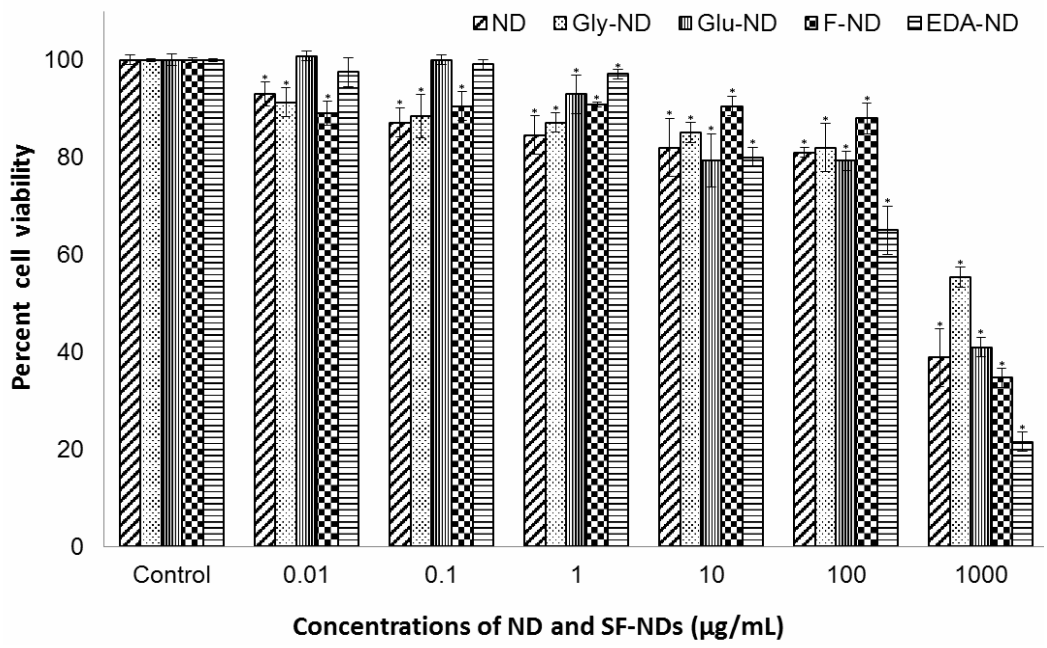

Figure 4. Cytotoxicity evaluation of Calu-3 cell lines after 24 h of incubation with nanodiamond (ND) and the surface functionalized nanodiamonds (SF-NDs). Error bars represent one standard deviation from the mean value (n = 3). Significant differences from control values are indicated by $*p < 0.05$.

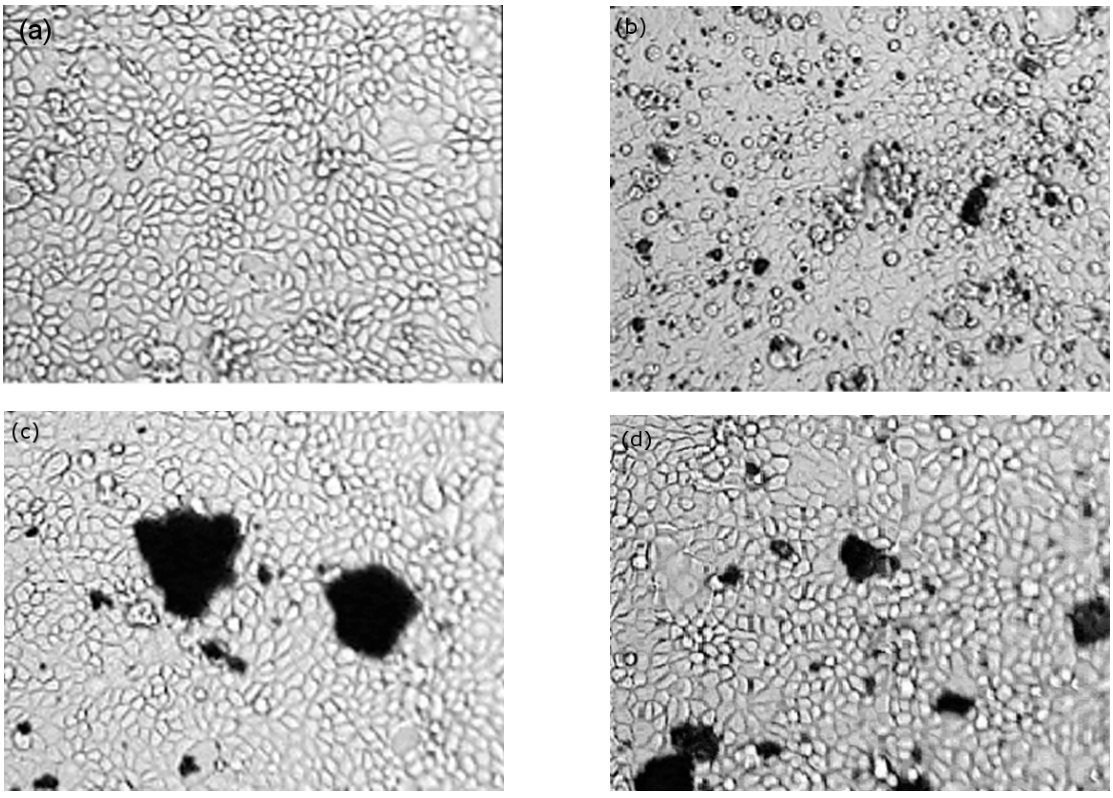

Figure 5

Figure 5 continued..

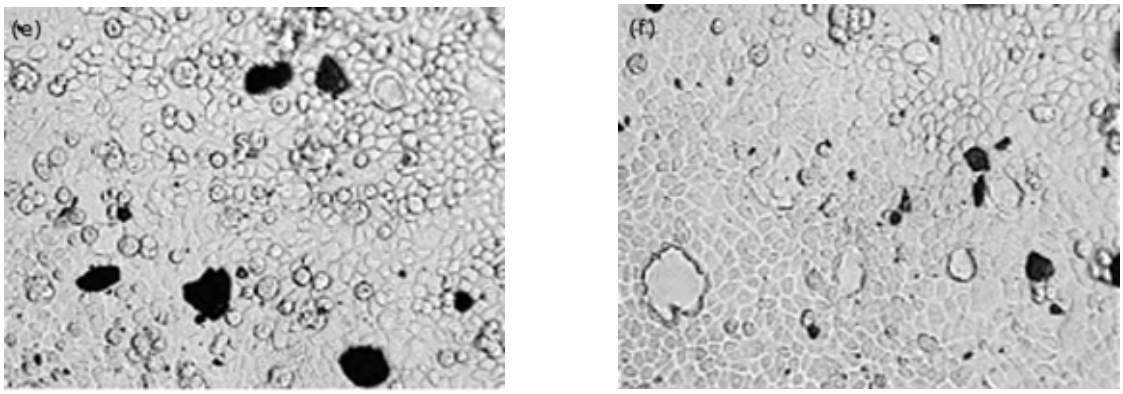

Figure 5. Morphological observation of Calu-3 cell lines (magnification x 100). a) control; and after 24 hrs exposure to 1000 μg/mL of b) ND; c) Gly-ND; d) Glu-ND; e) F-ND; and f) EDA-ND.

Table 2. Genes significantly up-regulated after ND exposure.

M	Fold change	Gene symbol	Gene title
1.850	3.606	*NQO1*	NAD(P)H dehydrogenase, quinone 1
1.585	3.000	*CNOT4*	CCR4-NOT transcription complex, subunit 4
1.379	2.602	*QKI*	quaking homolog, KH domain RNA binding (mouse)
1.260	2.395	*ZSCAN10*	zinc finger and SCAN domain containing 10
1.220	2.329	*THRSP*	thyroid hormone responsive (SPOT14 homolog, rat)
1.213	2.318	*PDE1A*	phosphodiesterase 1A, calmodulin-dependent
1.208	2.310	*PID1*	phosphotyrosine interaction domain containing 1
1.202	2.300	*FCHO2*	FCH domain only 2
1.089	2.127	*NIPBL*	Nipped-B homolog (*Drosophila*)
1.086	2.122	*VCAN*	versican
1.073	2.103	*SSPN*	sarcospan (Kras oncogene-associated gene)
1.071	2.100	*LOC641912*	hypothetical protein LOC641912 /// hypothetical LOC644090
1.011	2.016	*JAG1*	jagged 1 (Alagille syndrome)
0.994	1.992	*VPS13B*	vacuolar protein sorting 13 homolog B (yeast)
0.989	1.985	*BHLHB3*	basic helix-loop-helix domain containing, class B, 3
0.981	1.974	*PTPRH*	protein tyrosine phosphatase, receptor type, H
0.973	1.963	*SPTLC2*	serine palmitoyltransferase, long chain base subunit 2
0.972	1.962	*NRF1*	nuclear respiratory factor 1
0.962	1.948	*C16orf13*	chromosome 16 open reading frame 13
0.933	1.910	*IGLV2-14*	immunoglobulin lambda variable 2-14
0.920	1.892	*TOP3A*	topoisomerase (DNA) III alpha
0.916	1.886	*SGK2*	serum/glucocorticoid regulated kinase 2
0.907	1.876	*MRAS*	muscle RAS oncogene homolog
0.888	1.851	*CLCA2*	chloride channel, calcium activated, family member 2

Table 2 continued..

0.884	1.846	*C20orf67*	chromosome 20 open reading frame 67
0.878	1.838	*CDC2*	Cell division cycle 2, G1 to S and G2 to M
0.877	1.837	*TM9SF4*	transmembrane 9 superfamily protein member 4
0.866	1.823	*ZNF275*	zinc finger protein 275
0.862	1.818	*MKL1*	megakaryoblastic leukemia (translocation) 1
0.853	1.806	*SPTBN1*	Spectrin, beta, non-erythrocytic 1
0.842	1.793	*DGCR14*	DiGeorge syndrome critical region gene 14
0.832	1.781	*CDC27*	cell division cycle 27 homolog (*S. cerevisiae*)
0.832	1.780	*JPH1*	junctophilin 1
0.814	1.758	*FOXM1*	forkhead box M1
0.814	1.758	*PARP2*	poly (ADP-ribose) polymerase family, member 2
0.802	1.744	*LTB4DH*	leukotriene B4 12-hydroxydehydrogenase
0.802	1.743	*USP13*	ubiquitin specific peptidase 13 (isopeptidase T-3)
0.800	1.741	*KIF22*	kinesin family member 22 /// kinesin-like DNA-binding protein pseudogene
0.790	1.729	*SSFA2*	sperm specific antigen 2
0.790	1.729	*CXCR4*	chemokine (C-X-C motif) receptor 4
0.783	1.721	*KLC3*	kinesin light chain 3
0.776	1.713	*RAB27A*	RAB27A, member RAS oncogene family
0.773	1.709	*LOC149478*	Hypothetical protein LOC149478
0.755	1.688	*CDK2*	cyclin-dependent kinase 2
0.751	1.683	*BTRC*	beta-transducin repeat containing
0.742	1.673	*SAE1*	SUMO1 activating enzyme subunit 1
0.738	1.668	*DYRK1A*	dual-specificity tyrosine-(Y)-phosphorylation regulated kinase 1A

Table 3. Genes significantly down-regulated after ND exposure.

M	Fold change	Gene symbol	Gene title
-0.741	0.598	*FLJ10404*	hypothetical protein FLJ10404
-0.745	0.597	*KLC1*	kinesin light chain 1
-0.758	0.591	*C19orf33*	chromosome 19 open reading frame 33
-0.761	0.590	*PNRC2*	proline-rich nuclear receptor coactivator 2
-0.769	0.587	*C5orf41*	chromosome 5 open reading frame 41
-0.781	0.582	*RHBDD3*	rhomboid domain containing 3
-0.787	0.580	*SMAD5*	SMAD family member 5
-0.792	0.577	*FLJ22536*	hypothetical locus LOC401237
-0.796	0.576	*GUSBL2*	glucuronidase, beta-like 2
-0.826	0.564	*ID1*	inhibitor of DNA binding 1, dominant negative helix-loop-helix protein
-0.831	0.562	*KCTD12*	potassium channel tetramerisation domain containing 12
-0.834	0.561	*RC3H2*	ring finger and CCCH-type zinc finger domains 2
-0.836	0.560	*LRCH3*	leucine-rich repeats and calponin homology (CH) domain containing 3

Table 3 continued..

-0.840	0.559	*UNC13D*	unc-13 homolog D (*C. elegans*)
-0.859	0.551	*CHMP4B*	chromatin modifying protein 4B
-0.865	0.549	*SORBS3*	sorbin and SH3 domain containing 3
-0.871	0.547	*TBCD*	Tubulin folding cofactor D
-0.873	0.546	*C22orf32*	Chromosome 22 open reading frame 32
-0.887	0.541	*RUNX1*	runt-related transcription factor 1 (acute myeloid leukemia 1)
-0.897	0.537	*SPAG4L*	sperm associated antigen 4-like
-0.923	0.527	*NUDCD3*	NudC domain containing 3
-0.930	0.525	*MIA*	melanoma inhibitory activity
-0.930	0.525	*MSI2*	musashi homolog 2 (*Drosophila*)
-0.961	0.514	*ZFHX3*	zinc finger homeobox 3
-0.963	0.513	*ID3*	inhibitor of DNA binding 3, dominant negative helix-loop-helix protein
-0.972	0.510	*GABRA3*	gamma-aminobutyric acid (GABA) A receptor, alpha 3
-1.033	0.489	*ID4*	inhibitor of DNA binding 4, dominant negative helix-loop-helix protein
-1.044	0.485	*MAGI1*	membrane associated guanylate kinase, WW and PDZ domain containing 1
-1.049	0.483	*WNK1*	WNK lysine deficient protein kinase 1
-1.065	0.478	*USP36*	ubiquitin specific peptidase 36
-1.197	0.436	*CCAR1*	Cell division cycle and apoptosis regulator 1
-1.206	0.434	*NAALADL1*	N-acetylated alpha-linked acidic dipeptidase-like 1
-1.279	0.412	*MSI2*	musashi homolog 2 (*Drosophila*)
-1.281	0.411	*SOX4*	SRY (sex determining region Y)-box 4
-1.306	0.405	*TMEM134*	transmembrane protein 134
-1.440	0.369	*DDX17*	DEAD (Asp-Glu-Ala-Asp) box polypeptide 17
-1.440	0.369	*FNBP4*	formin binding protein 4
-1.528	0.347	*CAMK2N1*	calcium/calmodulin-dependent protein kinase II inhibitor 1
-1.692	0.310	*MALAT1*	metastasis associated lung adenocarcinoma transcript 1 (non-protein coding)

proteins and other vital organic molecules in the medium and induce indirect cytotoxic effects.

In a case of analytical separation technique, a potential selective adsorption of proteins and their immobilization onto surfaces of ND and SF-NDs may exert beneficial effects. Wei *et al.* [57] found that ND (3-10 nm) may serve as a support for protein identifying technique, and methods have been developed for capture and immobilization of cytochrome C [58] and glycoproteins on ND [59].

Microarray analysis

To elucidate the mechanism of cytotoxicity of the ND and SF-NDs, the gene expression profile of Calu-3 cells exposed to ND was examined to uncover the genes that were up-regulated (Table 2) or down-regulated (Table 3) and their possible correlation with the observed cytotoxic effect. As shown in Table 2, from the most significant genes assessed, the NAD(P)H dehydrogenase (*NQO1*) exhibited the greatest up-regulation (3.6-fold). On the contrary, the metastasis associated lung adenocarcinoma transcript 1 (*MALAT1*) displays the most significant down-regulation, 0.31-fold (Table 3). Guo *et al.* also demonstrated multi-walled carbon nanotubes altered gene expression of cancer-related genes [60].

Previously, Bakowicz-Mitura *et al.* showed that diamond powder particles influence gene expression and inhibit oxidative, cellular, and genotoxic stresses [61]. The results of the microarray study indicated that the response of Calu-3 cells to ND is subtle,

as only a few genes are affected more than 2-fold up or down.

CONCLUSION

This study reports on the physicochemical properties, cytotoxicity and gene expression profile of nanodiamonds and its derivatives on human lung derived cell lines (Calu-3). ND and the SF-NDs appear to be safe and biocompatible at concentration < 100 µg/mL. These observations are consistent with previous studies on other ND derivatives with other mammalian cell lines [45, 62]. The MTS assay and morphological evaluation provided evidence that ND and SF-NDs are cytotoxic at concentrations of 1000 µg/mL. The cytotoxicity of the studied samples was in the following order: EDA-ND > F-ND > ND Glu-ND > Gly-ND. Moreover, gene expression profile of Calu-3 cells exposed to ND indicated a minor change in gene expression.

ACKNOWLEDGEMENT

The support for this work was in part from University of Missouri System New Faculty Start up Fund to Dr. B. B. Youan and in part from Awards N RUE 2-2659-MO-05 and N RUE2-2894-TI-07 of the U.S. Civilian Research & Development Foundation (CRDF).

CONFLICT OF INTEREST STATEMENT

The authors declare no conflicts of interest.

REFERENCES

1. Yuejun, F., Na, A., Shuhua, Z., Aihua, L. and Yingqi, L. 2012, Diam. Relat. Mater., 21, 73.
2. Zhang, X., Lam, R., Xu, X., Chow, E. K., Kim, H. and Ho, D. 2011, Adv. Mater., 23, 4770.
3. Huang, H., Pierstorff, E., Osawa, E. and Ho, D. 2007, Nano. Lett., 7, 3305.
4. Merkel, T. J. and DeSimone, J. M. 2011, Sci. Transl. Med., 3, 73ps8.
5. Baker, M. 2010, Nat. Methods, 7, 957.
6. Fu, C. C., Lee, H. Y., Chen, K., Lim, T. S., Wu, H. Y., Lin, P. K., Wei, P. K., Tsao, P. H., Chang, H. C. and Fann, W. 2007, Proc. Natl. Acad. Sci. USA, 104, 727.
7. Hu, S. L., Bai, P. K., Sun, J. and Cao, S. R. 2010, Progress in Chemistry, 22, 345.
8. Pedro, V., Manoj, K. R., Humberto, G., Amrita, K., Venkat, B. and Ashok, K. 2011, Mater. Sci. Eng. C, 31, 1115.
9. Krueger, A. 2008, Chem. Eur. J., 14, 1382.
10. Beckerman, B. S., Jerrett, M., Finkelstein, M., Kanaroglou, P., Brook, J. R., Arain, M. A., Sears, M. R., Stieb, D., Balmes, J. and Chapman, K. 2012, Journal of Toxicology and Environmental Health-Part A-Current Issues, 75, 402.
11. Ghio, A. J., Carraway, M. S. and Madden, M. C. 2012, J. Toxicol. Env. Heal. B, 15, 1.
12. Liao, D., Shaffer, M. L., He, F., Rodriguez-Colon, S., Wu, R., Whitsel, E. A., Bixler, E. O. and Cascio, W. E. 2011, J. Toxicol. Env. Heal. A, 74, 693.
13. Pandolfi, M., Tobias, A., Alastuey, A., Sunyer, J., Schwartz, J., Lorente, J., Pey, J. and Querol, X. 2014, Sci. Total Environ., 494-495, 283.
14. Price, H. D., Arthur, R., BeruBe, K. A. and Jones, T. P. 2014, Atmos. Res., 147, 133.
15. Sanderson, P., Delgado-Saborit, J. M. and Harrison, R. M. 2014, Atmos. Environ., 94, 353.
16. Sarigiannis, D. A., Karakitsios, S. P., Kermenidou, M., Nikolaki, S., Zikopoulos, D., Semelidis, S., Papagiannakis, A. and Tzimou, R. 2014, Sci. Total Environ., 493, 795.
17. Bedeschi, E., Campari, C., Candela, S., Collini, G., Caranci, N., Frasca, G., Galassi, C., Francesca, G. and Vigotti, M. A. 2007, J. Toxicol. Env. Heal. A, 70, 261.
18. Kulkarni, N., Pierse, N., Rushton, L. and Grigg, J. 2006, N. Engl. J. Med., 355, 21.
19. Kalappanavar, N. K., Vinodkumar, C. S., Gouli, C., Sanjay, D., Nagendra, K., Basavarajappa, K. G. and Patil, R. 2012, Int. J. Occup. Environ. Med., 3, 68.
20. Cheng, M., Tsai, S., Chiu, H., Sung, F., Wu, T. and Yang, C. 2009, Inhal. Toxicol., 21, 1092.
21. Tsai, S., Chiu, H., Liou, S. and Yang, C. 2014, J. Toxicol. Env. Heal. A, 77, 1091.
22. Xing, Y., Xiong, W., Zhu, L., Osawa, E., Hussin, S. and Dai, L. 2011, Acs. Nano., 5, 2376.
23. Yokel, R. A. and MacPhail, R. C. 2011, J. Occup. Med. Toxicol., 6, 7.
24. Maynard, A. D., Aitken, R. J., Butz, T., Colvin, V., Donaldson, K., Oberdoerster, G., Philbert, M. A., Ryan, J., Seaton, A., Stone, V., Tinkle, S. S., Tran, L., Walker, N. J. and Warheit, D. B. 2006, Nature, 444, 267.

25. Bawa, R. 2011, Curr. Drug Delivery, 8, 227.
26. Huang, H. J., Chen, M., Bruno, P., Lam, R., Robinson, E., Gruen, D. and Ho, D. 2009, J. Phys. Chem. B, 113, 2966.
27. Dolmatov, V. Y. 2006, Applications of Detonation Nanodiamond, William Andrew Publishing, New York.
28. Kumar, A., Lin, P. A., Xue, A., Hao, B., Yap, Y. K. and Sankaran, R. M. 2013, Nature, 4, 2618.
29. Badziag, P., Verwoerd, W. S., Ellis, W. P. and Greiner, N. R. 1990, Nature, 343, 244.
30. Shenderova, O., Hens, S., Vlasov, I., Turner, S., Lu, Y., Van Tendeloo, G., Schrand, A., Burikov, S. A. and Dolenko, T. A. 2014, Part. Part. Syst. Char., 31, 580.
31. Gogotsi, Y., Welz, S., Ersoy, D. A. and McNallan, M. J. 2001, Nature, 411, 283.
32. Chen, M., Pierstorff, E. D., Lam, R., Li, S. Y., Huang, H., Osawa, E. and Ho, D. 2009, Acs. Nano., 3, 2016.
33. Lam, R. and Ho, D. 2009, Expert Opin. Drug Del., 6, 883.
34. Li, J., Zhu, Y., Li, W., Zhang, X., Peng, Y. and Huang, Q. 2010, Biomaterials, 31, 8410.
35. Smith, A. H., Robinson, E. M., Zhang, X., Chow, E. K., Lin, Y., Osawa, E., Xi, J. and Ho, D. 2011, Nanoscale, 3, 2844.
36. Martin, R., Alvaro, M., Herance, J. R. and Garcia, H. 2010, Acs. Nano., 4, 65.
37. Kaur, R., Chitanda, J. M., Michel, D., Maley, J., Borondics, F., Yang, P., Verrall, R. E. and Badea, I. 2012, Int. J. Nanomed., 7, 3851.
38. Kakran, M. and Li, L. 2012, Materials Integration, 508, 76.
39. Kaur, R. and Badea, I. 2013, Int. J. Nanomed., 8, 203.
40. Khabashesku, V. N., Margrave, J. L. and Barrera, E. V. 2005, Diamond Relat. Mater., 14, 859.
41. Osswald, S., Yushin, G., Mochalin, V., Kucheyev, S. O. and Gogotsi, Y. 2006, J. Am. Chem. Soc., 128, 11635.
42. Vaijayanthimala, V. and Chang, H. C. 2009, Nanomedicine, 4, 47.
43. Hamers, R. J. 2008, Nature, 454, 708.
44. Huang, S., Shao, J., Gao, L., Qi, Y. and Ye, L. 2011, Appl. Surf. Sci., 257, 8617.
45. Liu, K. K., Wang, C. C., Cheng, C. L. and Chao, J. I. 2009, Biomaterials, 30, 4249.
46. Shimkunas, R. A., Robinson, E., Lam, R., Lu, S., Xu, X., Zhang, X. Q., Huang, H., Osawa, E. and Ho, D. 2009, Biomaterials, 30, 5720.
47. Zhang, X., Yin, J., Kang, C., Li, J., Zhu, Y., Li, W., Huang, Q. and Zhu, Z. 2010, Toxicol. Lett., 198, 237.
48. Chen, Y., Lee, D., Hsiao, C., Chung, Y., Chen, H., Thomas, J. P., Pong, W., Tai, N., Lin, I. and Chiu, I. 2009, Biomaterials, 30, 3428.
49. Schrand, A. M., Huang, H. J., Carlson, C., Schlager, J. J., Osawa, E., Hussain, S. M. and Dai, L. M. 2007, J. Phys. Chem. B, 111, 2.
50. Yu, S. J., Kang, M. W., Chang, H. C., Chen, K. M. and Yu, Y. C. 2005, J. Am. Chem. Soc., 127, 17604.
51. Yuan, Y., Wang, X., Jia, G., Liu, J. H., Wang, T. C., Gu, Y. Q., Yang, S. T., Zhen, S., Wang, H. F. and Liu, Y. F. 2010, Diamond Relat. Mater., 19, 291.
52. Liu, Y., Gu, Z., Margrave, J. L. and Khabashesku, V. N. 2004, Nanodiamond Derivatives, 16, 3924.
53. Ding, L. H., Stilwell, J., Zhang, T. T., Elboudwarej, O., Jiang, H. J., Selegue, J. P., Cooke, P. A., Gray, J. W. and Chen, F. Q. F. 2005, Nano. Letters, 5, 2448.
54. Murdock, R. C., Braydich-Stolle, L., Schrand, A. M., Schlager, J. J. and Hussain, S. M. 2008, Toxicol. Sci., 101, 239.
55. Pouchert C. 1981, The Aldrich Library of Infrared Spectra, Aldrich Chemical Co., Milwaukee, WI.
56. Casey, A., Herzog, E., Lyng, F. M., Byrne, H. J., Chambers, G. and Davoren, M. 2008, Toxicol. Lett., 179, 78.
57. Wei, L. M., Xue, Y., Zhou, X. W., Jin, H., Shi, Q., Lu, H. J. and Yang, P. Y. 2008, Talanta, 74, 1363.
58. Huang, L. C. and Chang, H. C. 2004, Langmuir, 20, 5879.
59. Yeap, W. S., Tan, Y. Y. and Loh, K. P. 2008, Anal. Chem., 80, 4659.
60. Guo, N. L., Wan, Y., Denvir, J., Porter, D. W., Pacurari, M., Wolfarth, M. G., Castranova, V. and Qian, Y. 2012, J. Toxicol. Env. Heal. A, 75, 1129.
61. Bakowicz-Mitura, K., Bartosz, G. and Mitura, S. 2007, Surf. Coat. Technol., 201, 6131.
62. Thalhammer, A., Edgington, R. J., Cingolani, L. A., Schoepfer, R. and Jackman, R. B. 2010, Biomaterials, 31, 2097.